On the Detection and Identification of Cosmic Gamma-rays in a Cosmic Ray Detector

Jin Chang[1,2], W.K.H. Schmidt[1], Opher Ganel[3], Eun-Suk Seo[3], Ramin Sina[3], Jian-Zhong Wang[3]
For the ATIC Collaboration
[1] *Max-Planck-Institut für Aeronomie, D-37191 Katlenburg-Lindau, Germany*
[2] *Purple Mountain Observatory, Academia Sinica, Nanjing, China*
[3] *Institute for Physical Science and Technology, University of Maryland, College Park, MD20742*

Abstract

As very high energy gamma-rays (10 GeV to 100 TeV) can provide clues to the origin of the highest energy cosmic radiation, new VHE gamma-ray observations are very desirable. For the near-to-intermediate future a number of cosmic ray detector projects are being planned. We have investigated the possibility of detecting gamma-rays with these type detectors by simulating the nuclear-electromagnetic shower development in heavy materials with the GEANT computer code. Using as an example the Advanced Thin Ionization Calorimeter (ATIC), we have developed an algorithm to reject the high flux of charged particle background by studying the three-dimensional shape of the shower in a fully active calorimeter.

1 Introduction

For the near-to-intermediate future a number of cosmic ray detector projects are being planned. In order to get the most out of a specific experiment, it is often attempted to add to the basic configuration (pertaining to a specific goal) special features that allow some kind of optimization for secondary goals. We have made an attempt to look at the problem in a different way: We propose to accept the design of a cosmic ray detector as it is optimized for a specific purpose, and see what can be done for secondary goals without any attempt to add features or changing the design in any way. As we are involved in the Advanced Thin Ionization Calorimeter (ATIC) balloon experiment we have taken that one as an example. ATIC is dedicated to the observation of primary protons and heavy nuclei, and by simulation calculations, using the computer code GEANT3.21, we have tried to find out how well high energy gamma-rays can be measured with the design as it is. In an accompanying paper at this conference (Schmidt, et al., 1999) we do the same for the identification of high energy electrons in the same instrument.

To date there are no instruments dedicated to observations of gamma-rays in the energy range between the EGRET detector (sensitive below 30 GeV) on the Compton Gamma-ray Observatory (CGRO) and ground based Cherenkov detectors (sensitive above 500 GeV). GLAST (Bloom, 1996) has been proposed for a new high energy gamma-ray telescope, its energy range is from 20 MeV to 300 GeV. Cosmic-ray instruments, however, feature large area, wide field of view and long observing time . In this paper we discuss the possibility of using these detectors to observe gamma-rays in the energy range from 20 GeV to 1000 GeV.

2 ATIC Configuration

A detailed description of the ATIC experiment is provided elsewhere in these proceedings (Guzik, et al., 1999; Ganel, et al., 1999) therefore a brief description of the main features of the instrument will suffice here. The detector contains three main components: charge module, target, and all active BGO calorimeter. The Charge module is located at the top of the instrument and is composed of a solid state silicon matrix detector. The target includes 30 cm of graphite (1.6 radiation lengths or 0.75 interaction lengths) arranged in three 10 cm thick layers with scintillators, each consisting of two crossed layers of 2cm wide by 1cm thick strips. The calorimeter is composed of an array of BGO crystals, each 2.5 cm x 2.5 cm x 25 cm, layered horizontally with 40 crystals forming a 50 cm x 50 cm layer; alternate layers are rotated 90 degrees with respect to each other.

A typical gamma-ray event passes first through the charge module, then interacts in the target and finally develops a shower in the BGO calorimeter.

3 Background Rejection

The measurement of charged cosmic-rays is the main objective for the ATIC detector, but such events constitute background for gamma-ray observing. A very efficient anticoincidence system is required to reject the much higher flux of charged cosmic rays. In very high energy gamma-ray observing, if one would use an integral scintillator to act as an anticoincidence system, many real gamma-rays will be rejected because of backscattering from the very intense electron-photon shower in the calorimeter. Our simulation results shows that at 1TeV photon energy, about 50% of the incident gamma-rays would be lost.

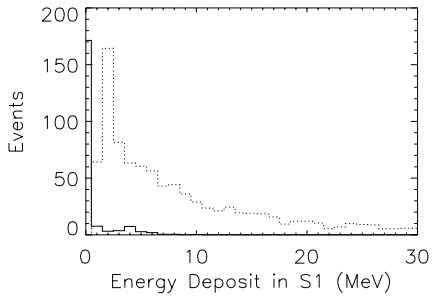

Figure 1: Distributions of energy deposit in the first scintillator for 90 - 110 GeV gamma-rays (solid curve, reduced 5-fold), and 90 - 100 GeV (BGO energy deposit value) protons (dashed curve).

For gamma-ray detection in ATIC, the charge module is used as an anticoincidence system in off-line data analysis. Since backscattering from the shower in the calorimeter is almost isotropic, we can choose several strips around the incident trajectory to act as anticoincidence. The detection efficiency and background level depend on the number of strips chosen to reject background; this number is determined by trajectory resolution.

3.1 Trajectory Determination For the reconstruction of the incident trajectory we have developed an algorithm (Seo, 1996) to determine the primary trajectory from the projection of the cascade core as measured by the crossed (x,y) BGO crystals in the calorimeter. From the calculated energy deposit distribution in each BGO layer, the position of the maximum energy deposit can be determined. From this, the trajectory can be calculated and its crossing position in the charge module determined. We have studied the positional resolution for proton trajectories in the top scintillator and found that this distribution has wide wings as compared to the attempted Gaussian fit. From this distribution it is difficult to determine the number of strips around the impact position that is necessary to be used as an anticoincidence area for the identification of incident gamma rays. But for real gamma-ray events, this distribution looks different, the width is smaller and there are no conspicuous wings in this distribution.

3.2 Differences Between Gamma-ray and Hadron Showers in ATIC

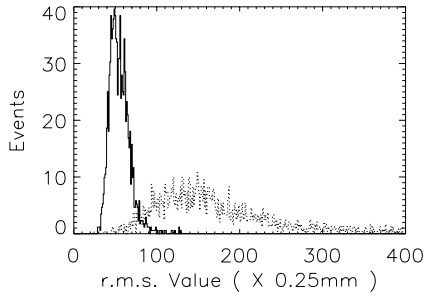

Figure 2: The r.m.s. width distribution of energy deposit in the second BGO layer for 90 - 110 GeV gamma-rays (solid curve) and 90 - 110 GeV (total BGO energy deposit) protons (dashed curve).

It is well known that showers resulting from gamma-ray conversions have different properties from those caused by hadrons. By observing the pattern of charged particle 'hits' in the scintillator and silicon matrix array and the energy deposit pattern in the calorimeter, events caused by gamma-rays can be distinguished from the much more frequent hadrons by the following criteria:

1) Energy deposit distribution in the first scntillator: Figure 1 shows the energy deposit distribution in the top scintillator for 1000 gamma-rays having energy 90 -110 GeV and 1000 proton events depositing 90 - 110 GeV in the BGO. Since most backscattered particles from gamma-ray showers are photons, their average energy deposit in the top scintillator are much lower than that of protons.

2) R.M.S. of the energy deposit distribution in the BGO calorimeter: We use the r.m.s. value to describe the lateral extent of a shower in an individual BGO layer. Figure 2 shows the r.m.s. distribution of 1000 events each of 90 - 110 GeV gamma-rays and 90-110 GeV (total energy deposit) protons in the second BGO layer. One

can see that hadron induced showers are on average much wider in lateral size than the showers caused by gamma-rays.

3) Energy deposit and r.m.s. in the last BGO layer: In Figure 3 we show a scatter plot of the ratio of the fraction of total energy deposited in BGO layer 10 vs the r.m.s. widthof the deposit pattern there. Dots represent 1000 gamma-ray events at 90 - 110 GeV and crosses represent protons with the same total energy deposit. We define a function that allows us to make use of the fact that the two populations are clearly separated, (but not simply in either energy deposit or r.m.s. value alone):$\mathbf{F} = \frac{En}{Sum} r.m.s.^2$, where En is the energy deposit in the last BGO layer and Sum is total energy deposit in the BGO calorimeter. The result shows that F is a good parameter to distinguish gamma-rays from protons in this bottom BGO layer. About 99% proton would be rejected by it.

3.3 Background Level of Gamma-ray Observing in ATIC According to the difference between gamma-ray and hadron showers we have developed an algorithm to select proton events which look like gamma-ray events. This algorithm rejects about 99.5% of the proton events. For the remaining 'gamma-ray like' events the trajectory resolution is much better than for all proton events. The uncertainty of the impact position in the first scintillator is improved from 3.5 cm to 1.8 cm (r.m.s.), and the distribution of calculated impact positions does not have large wings which looks like the normal distribution. We compare the signal in, e.g., seven 2 cm wide scintillator strips around the calculated impact position with the signal expected from a minimum ionizing particle. The probability of a proton generating a lower (or zero) signal there is about 10^{-4} separately for either X or Y. This can serve as a local anti-coincidence veto. The probabilities for both dimensions, X and Y, are not correlated (linear correlation coefficient is less than 0.1) so the rejection power can be multiplied. This yields (for the top X,Y pair of scintillator layers) a total rejection power of 10^{-8} for the 0.5% of 'gamma-ray-like' protons after the shower selection described above. Therefore, using the shower characteristics as described above plus what we might call the 'localized anticoincidence system' as described in this paragraph, results in misidentifying one proton event in about 2×10^{10} as a gamma-ray event. If confirmed by calibration measurements this is sufficient to observe cosmic gamma-rays at high energies with this particular cosmic ray detector (ATIC)

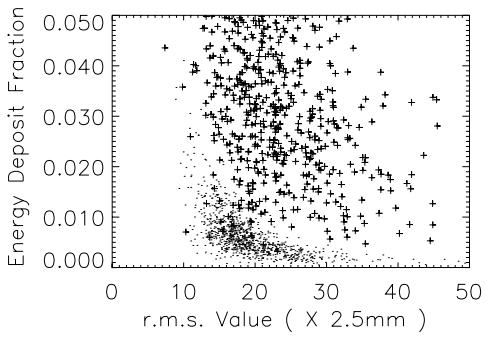

Figure 3: Fractional energy deposit in BGO layer 10 vs. r.m.s. width in that layer for 90 - 110 GeV gamma-rays (dots) and 90 - 110 GeV protons (plus signs).

The relation between the number of strips which would act as anticoincidence, background level and detection efficiency is listed in the table below. It can be seen that the calculation results tally with simulation results very well.

Number Of Strips	3	5	7	9
BLbyCal[1]	5×10^{-4}	2.5×10^{-5}	5×10^{-7}	2.8×10^{-9}
BLbySimu[1]	24/50000	3/50000	0/50000	0/50000
DeteEffi[1]	55.6%	43.6%	42.2%	41.2%
BLbyCal[2]	4×10^{-5}	1.47×10^{-7}	5×10^{-11}	3.4×10^{-16}
BLbySimu[2]	4/50000	$<$ 1/50000	$<$ 1/50000	$<$ 1/50000
DeteEffi[2]	43.6%	42.1%	39.8%	36.8%

BLbyCal[1] Background level by calculation for one layer scintillator to act as anticoincidence system
BLbySimu[1] Background level by simulation for one layer scintillator to act as anticoincidence system
DeteEffi[1] Detection efficiency at 1 TeV for one layer scintillator to act as anticoincidence system
BLbyCal[2] Background level by calculation for two layer scintillators to act as anticoincidence system

BLbySimu^2 Background level by simulation for two layer scintillators to act as anticoincidence system
DeteEffi^{2}Detection efficiency at 1 TeV for two layer scintillators to act as anticoincidence system

4 Expected Performance of Gamma-ray Detection in ATIC

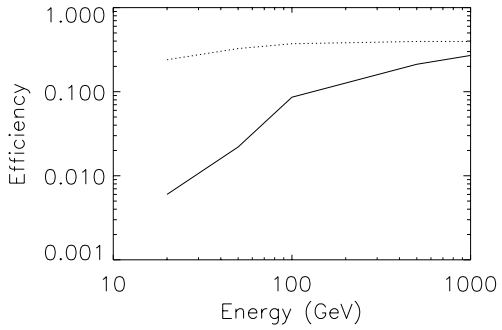

Figure 4: Energy dependence of detection efficiency for Model.1 (solid curve) and Model.2 (dashed curve).

The mean energy deposition of photons is about 97% of the incident energy, almost independent of the incident energy. The energy resolution varies from 3.1% to 1.7% below 100 GeV, and it is almost constant from 100 GeV to 1 TeV. The detection efficiency depends on different assumed trigger models. Model 1 is that there must be at least 0.5 MeV energy deposition in the first Scintillator (charged particle trigger, normal CR operation), Model 2 assumes that there is no such minimum required. Figure 4 shows how the detection efficiency (with two layer scintillator anticoncidence system, each layer 7 strips) depends on energy for the different models. For Model 1 and Model 2 at 1 TeV, the detection efficiency is about 28% and 40% , respectively. The angular resolution of the arrival direction for an isotropic photon flux is better than 1.6 degrees. This is important for the observation of celectial gamma-ray sources.

5 Summary

For gamma-ray observing, ATIC can measure the energy, trajectory and arrival direction of the incident photons. Its energy resolution is much higher than and the angular resolution is comparable to that of ground-based instruments (Vacanti,1991, and Weekes, 1989). Even though the main objective of ATIC is charged cosmic ray observations, the detection effciency for gamma-rays (about 30%) is better than intuitively expected, and the effective area is greater than 1000 cm^2 for vertically incident photons.

For the near-to-intermediate future a number of cosmic ray detector projects are being planned. We have shown that such detectors can be used to observe gamma-rays without compromising their main objective.

ATIC will probably not be able to observe celestial gamma rays. At the minimum balloon flight altitude required for hadron and nuclei observations the atmospheric gamma-ray background is too high to observe diffuse cosmic gamma radiation, and for the long duration flights (e.g. over Antarctica) there are likely no particularly strong cosmic gamma-ray sources within the field of view. But the basic principle of gamma-ray identification can be verified, and while the balloon is drifting somewhat up and down in altitude, it may be possible to determine the atmospheric background flux up to fairly high photon energies.

References

Bloom, E.D., Sp. Sci. Rev., 75, 109, 1996
Ganel, O., et al., OG 4.6.01, Proc. 26th ICRC (Salt Lake City, 1999)
Guzik, T. G., et al., OG 4.1.03, Proc. 26th ICRC (Salt Lake City, 1999)
Seo, E.S., et al., Proc. SPIE (Colorado), 2806, 134, ed D.Ramsey & T.A.Parnell (1996)
Vacanti, G., et al., 1991, ApJ, 377, 467
Weekes, T.C., et al., 1989, ApJ, 342, 379
W.K.H. Schmidt, et al., OG 4.1.11, Proc. 26th ICRC (Salt Lake City, 1999)